

STAR FORMATION AND DUST OBSCURATION AT  $Z \approx 2$ : GALAXIES AT THE DAWN OF DOWNSIZING\*

M. PANNELLA<sup>1</sup>, C. L. CARILLI<sup>1</sup>, E. DADDI<sup>2</sup>, H. J. MC CRACKEN<sup>3</sup>, F. N. OWEN<sup>1</sup>, A. RENZINI<sup>4</sup>, V. STRAZZULLO<sup>1</sup>,  
 F. CIVANO<sup>5</sup>, A. M. KOEKEMOER<sup>6</sup>, E. SCHINNERER<sup>7</sup>, N. SCOVILLE<sup>8</sup>, V. SMOLČIĆ<sup>8</sup>, Y. TANIGUCHI<sup>9</sup>, H. AUSSEL<sup>2</sup>,  
 J. P. KNEIB<sup>10</sup>, O. ILBERT<sup>11,12</sup>, Y. MELLIER<sup>3</sup>, M. SALVATO<sup>8</sup>, D. THOMPSON<sup>13</sup>, C. J. WILLOTT<sup>14</sup>.

## ABSTRACT

We present first results of a study aimed to constrain the star formation rate and dust content of galaxies at  $z \approx 2$ . We use a sample of BzK-selected star-forming galaxies, drawn from the COSMOS survey, to perform a stacking analysis of their 1.4 GHz radio continuum as a function of different stellar population properties, after removing AGN contaminants from the sample. Dust unbiased star formation rates are derived from radio fluxes assuming the local radio-IR correlation. The main results of this work are: i) specific star formation rates are constant over about 1 dex in stellar mass and up to the highest stellar mass probed; ii) the dust attenuation is a strong function of galaxy stellar mass with more massive galaxies being more obscured than lower mass objects; iii) a single value of the UV extinction applied to all galaxies would lead to grossly underestimate the SFR in massive galaxies; iv) correcting the observed UV luminosities for dust attenuation based on the Calzetti recipe provide results in very good agreement with the radio derived ones; v) the mean specific star formation rate of our sample steadily decreases by a factor of  $\sim 4$  with decreasing redshift from  $z = 2.3$  to 1.4 and a factor of  $\sim 40$  down the local Universe.

These empirical SFRs would cause galaxies to dramatically overgrow in mass if maintained all the way to low redshifts, we suggest that this does not happen because star formation is progressively quenched, likely starting from the most massive galaxies.

*Subject headings:* galaxies: evolution — galaxies: luminosity function, mass function — galaxies: fundamental parameters — galaxies: statistics — galaxies: ISM — surveys

## 1. INTRODUCTION

How and when galaxies build up their stellar mass is still a major question in observational cosmology. While a general consensus has been reached in the last years on the evolution of the galaxy stellar mass function (e.g. Dickinson et al. 2003; Drory et al. 2004; Bundy et al. 2005; Pannella et al. 2006; Fontana et al. 2006; Marchesini et al. 2008), the red-

shift evolution of the star formation rate as a function of stellar mass  $SFR(M, z)$  still remains unclear. Several studies, mainly based on UV derived SFR, have found the persistence of the, locally well established, anticorrelation between specific star formation rate and stellar mass up to high redshift (e.g. Juneau et al. 2005; Feulner et al. 2005; Bauer et al. 2005; Erb et al. 2006; Noeske et al. 2007; Zheng et al. 2007; Cowie & Barger 2008; Damen et al. 2009; Davies et al. 2009). This anticorrelation is often regarded in the literature as a manifestation of the "downsizing" scenario (Cowie et al. 1996), whereby more massive galaxies form at higher redshift. Part of this effect is certainly real, as for  $z < 2$  the most massive galaxies tend to be passively evolving ellipticals with no or little ongoing star formation. However, when referring to actively star forming galaxies alone whether this anticorrelation exists or not depends on the way SFRs are estimated. As already warned by Cowie et al. (1996), one important and poorly known ingredient in deriving SFRs from rest-frame UV fluxes is the amount of dust attenuation suffered by the UV light in the inter-stellar medium. Lacking spectral information for large samples, the dust attenuation factor is the result of a multi-parameter, and highly degenerate, fitting to the multiwavelength photometry available or, when the photometric coverage is not sufficient, a median factor is applied to the whole galaxy sample.

An independent estimate of the star formation rate in a galaxy, not biased by the galaxy's dust content, is provided by its radio continuum emission. This is due to processes, the free-free emission from HII regions and the synchrotron radiation from relativistic electrons, dominated by young massive stars. By mean of the well established (but not as well understood) radio-FIR correlation (e.g. Condon 1992; Kennicutt 1998; Yun et al. 2001) it is possible to estimate the total star formation rate in a galaxy from its radio luminosity. Thanks to their arcsecond resolution and relatively wide field of view, radio interferometric observations offer several advantages over

\* Based on observations collected, within the COSMOS Legacy Survey, at the HST, Chandra, XMM, Keck, NRAO-VLA, Subaru, KPNO, CTIO, CFHT and ESO observatories. The National Radio Astronomy Observatory is a facility of the National Science Foundation operated under cooperative agreement by Associated Universities, Inc.

<sup>1</sup> National Radio Astronomy Observatory, P.O. Box 0, Socorro, NM 87801-0387; mpannell@nrao.edu

<sup>2</sup> CEA, Laboratoire AIM - CNRS - Université Paris Diderot, Irfu/SAP, Orme des Merisiers, F-91191 Gif-sur-Yvette, France.

<sup>3</sup> Institut d'Astrophysique de Paris, 98 bis Boulevard Arago, 75014 Paris, France.

<sup>4</sup> INAF - Osservatorio Astronomico di Padova, Vicolo dell'Osservatorio 5, I-35122 Padova, Italy.

<sup>5</sup> Harvard Smithsonian Center for Astrophysics 60 Garden Street, MS 67 Cambridge, MA 02138.

<sup>6</sup> Space Telescope Science Institute 3700 San Martin Drive, Baltimore MD 21218.

<sup>7</sup> Max Planck Institut für Astronomie, Königstuhl 17, Heidelberg, D-69117, Germany.

<sup>8</sup> California Institute of Technology, MS 105-24, Pasadena, CA 91125.

<sup>9</sup> Graduate School of Science and Engineering, Ehime University, Bunkyo-cho, Matsuyama 790-8577, Japan.

<sup>10</sup> Laboratoire d'Astrophysique de Marseille, Technopôle de Marseille-Etoile 38, rue Frédéric Joliot-Curie 13388 Marseille cedex 13 FRANCE

<sup>11</sup> Institute for Astronomy, 2680 Woodlawn Dr., University of Hawaii, Honolulu, Hawaii, 96822

<sup>12</sup> Laboratoire d'Astrophysique de Marseille, BP 8, Traverse du Siphon, 13376 Marseille Cedex 12, France

<sup>13</sup> Large Binocular Telescope Observatory U.of.A, 933 N. Cherry Ave. Tucson, AZ

<sup>14</sup> Herzberg Institute of Astrophysics, National Research Council, 5071 West Saanich Rd, Victoria, BC V9E 2E7, Canada

present-day FIR facilities which are limited by their  $\sim 10''$  resolution and narrow field of view. For this very reason radio continuum observations turn out to be an excellent tool for tracing the dust-unobscured star formation in the high redshift Universe.

However, radio emission is not only produced by star formation but also by AGN, and therefore a major challenge in deriving dust-unbiased SFRs from radio fluxes is to remove the AGN contamination (e.g. Smolčić et al. 2008). At  $z > 1$ , even in the deepest present-day surveys, radio detections are likely to include a substantial population of AGNs, although extreme ULIRG/SMG-like starbursting galaxies do exist. Therefore the best way to explore, with existing radio facilities, the dust-unbiased SFRs of normal galaxy populations is to use a stacking analysis of the radio data, which allows the investigation of large galaxy samples drawn from optical-NIR surveys that are individually undetected in the radio. This technique has been already used in a number of radio studies (e.g. Daddi et al. 2007a; White et al. 2007; Carilli et al. 2007, 2008; Dunne et al. 2009; Garn & Alexander 2009).

In this context the Cosmic Evolution Survey (COSMOS, Scoville et al. 2007), with its state-of-the-art multiwavelength coverage all the way from X-rays to radio of a  $2\Omega^\circ$  field provides an ideal opportunity to build large high redshift galaxy samples with well characterized spectral properties. We take advantage of the COSMOS database to select a large sample of  $1 < z < 3$  star-forming galaxies, and derive dust-unbiased SFRs from stacking the 1.4 GHz radio data.

Throughout this paper we use AB magnitudes and adopt a  $\Lambda$  cosmology with  $\Omega_M = 0.3$ ,  $\Omega_\Lambda = 0.7$  and  $H_0 = 70 \text{ km s}^{-1} \text{ Mpc}^{-1}$ .

## 2. RADIO, OPTICAL, NEAR INFRARED AND X-RAY DATA

Here we use the VLA medium-deep 1.4GHz imaging covering the whole COSMOS field with a fairly uniform rms ( $\approx 10 \mu\text{Jy}$ ) and an angular resolution of  $1.5''$  (see Schinnerer et al. 2007).

Deep SUBARU  $B, z$  imaging (Capak et al. 2007) and CFHT  $K_s$ -band data (McCracken et al. 2009, submitted) were used to select a dust-unbiased sample of about 34,000 star-forming BzK galaxies (sBzK, see left panel of Figure 1) with  $K_s < 23$ . We refer to McCracken et al for a detailed description of the  $K$ -selected BzK sample. Following Daddi et al. (2004) galaxy stellar masses were estimated assuming a Salpeter (1955) initial mass function from 0.1 to  $100 M_\odot$ . A photometric redshift was assigned to more than 80% of the sBzK sample, by cross-correlating with the COSMOS photometric redshift catalog by Ilbert et al. (2009). The median photo- $z$  is  $\sim 1.7$ , with less than 2% of the sample at redshift lower than 1 or higher than 3 (see right panel of Figure 1), confirming the effectiveness of the BzK selection technique.

A small fraction ( $\approx 2\%$ ) of the sBzK sample has a 1.4GHz counterpart. The minimum flux density of the radio counterparts, corresponding to a  $3\sigma$  detection, is about  $30 \mu\text{Jy}$  which, at a median redshift of 1.7, corresponds to a radio luminosity of about  $5 \times 10^{23} \text{ W/Hz}$  at 1.4GHz.

In the local Universe it is usually assumed, based on radio luminosity function studies (e.g. Sadler et al. 2002; Condon et al. 2002), that 1.4GHz radio luminosities greater than  $\approx 2 \times 10^{23} \text{ W/Hz}$  are mostly produced by AGNs, while below this luminosity star formation has a dominant role in producing the observed radio emission, maybe still in concurrence with a low-luminosity AGN. Even though recent studies (e.g. Smolčić et al. 2009ab; Strazzullo et al., in preparation) are

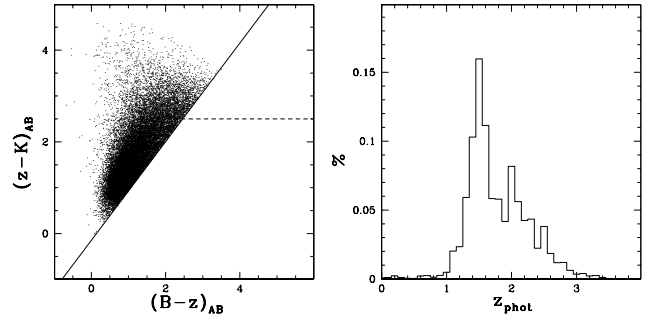


FIG. 1.— **Left:** The selection diagram for sBzK star forming galaxies at  $z \approx 2$ . **Right:** Photometric redshift distribution of the COSMOS sBzK sample. The bulk of the sample spans the redshift range [1.3-2.5].

suggesting that such a characteristic luminosity was brighter at higher redshift, the sBzK radio detections are mostly *extreme* objects: AGN dominated galaxies or SMG-like starbursts.

In order to study star formation and dust content for the *normal* galaxy population, mostly undetected in radio, we removed from the sample all the objects with a radio counterparts. In doing so we are likely removing, along with AGN dominated sources, also the tail of extreme star forming objects. Nonetheless we prefer this conservative approach in order to derive more robust conclusions.

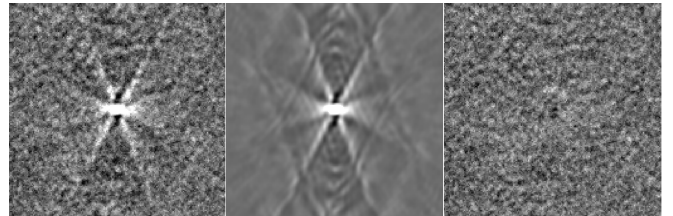


FIG. 2.— **Left:** Median stacking result of all the 34000 sBzK galaxies. **Mid-** **dle:** Best fit dirty beam convolved Gaussian to the stacked data. The total flux recovered is  $8.8 \pm 0.1 \mu\text{Jy}$ . **Right:** Residual image.

In a further attempt to remove AGN contributed radio emission, we restrict our analysis to the inner central 0.9 square degree of the COSMOS field, which is covered by deep Chandra observations (Elvis et al. 2009). The depth of the Chandra survey reaches  $1.9 \times 10^{-16} \text{ erg cm}^{-2} \text{ s}^{-1}$ , in the soft band (0.5-2keV), which at the median redshift of our sample allows an important census of the AGN luminosity function. We cross-correlated the sBzK sample with the catalog of Chandra counterparts (Civano et al. 2009, submitted), removing all matched sources (575) from the final catalog.

Excluding individually-detected X-ray sources may not completely eliminate AGN sources from the sample. Indeed, sBzK galaxies with a mid-IR excess ( $\sim 20-30\%$  of the total) are likely to contain heavily obscured (Compton thick) AGNs, as indicated by their X-ray stacking (Daddi et al. 2007b). However, mid-IR excess and non-excess (normal) galaxies exhibit quite similar 1.4 GHz radio properties (Daddi et al. 2007a), suggesting that such Compton-thick AGNs do not contribute substantially to the radio flux at 1.4 GHz. Moreover, our median stacking technique automatically reduces the impact of a minority of galaxies with radio emission in excess from what is expected from star formation, if they exist.

We ended up with a reduced sample of 11798 objects, over an area of  $\approx 0.9$  square degrees, with a photometric redshift in the range  $1 < z < 3$  and having removed both the radio (248) and the Chandra (575) detections. In the following we will

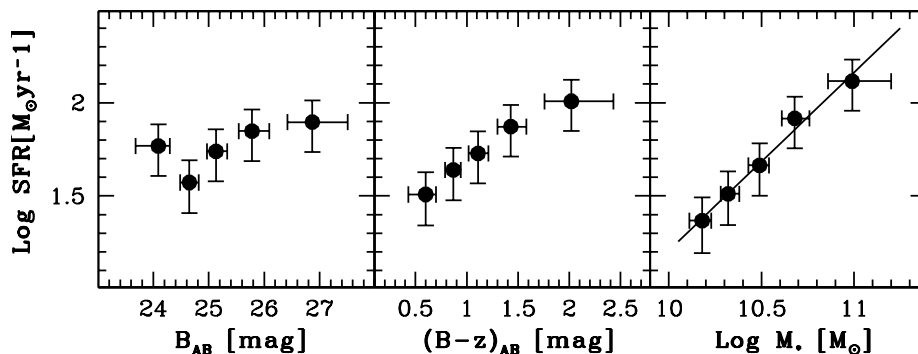


FIG. 3.— Total radio-derived SFR versus B band (left), B-z color (middle), and stellar mass (right). The solid line is the best fit line:  $\text{Log}(\text{SFR}) \propto 0.95 \text{Log} M_*$ .

present results based on this sub-sample but even analyzing the full sBzK sample our conclusions would remain substantially the same.

### 3. DATA ANALYSIS AND RADIO-DERIVED SFR

For each of these sBzK sources, we produced a cutout in the radio mosaic of  $173 \times 173 \text{ pixel}^2$  ( $60.5 \times 60.5 \text{ arcsec}^2$ ). These cutouts were then stacked to create median images. Median stacking is more robust than mean against the tails of the distribution, while the rms still goes down by  $\approx \sqrt{N}$ . Stacking images allows an easy way to treat the Bandwidth Smearing (BWS) effect. This is a well known instrumental effect in aperture synthesis astronomy (see Thompson 1999), consisting of a radial stretching of the sources in the image due to the finite width of the frequency response of the receiver. The BWS does not affect the total flux of the source though. Total fluxes are retrieved by fitting a dirty beam convolved with a Gaussian function to the stacked data. The Galfit code (Peng et al. 2002) was used for this purpose, but very similar results were obtained using the AIPS/CLEAN algorithm. As an example, in Figure 2 we show the stacked data, model and residual image for the original whole (34,000 galaxies) sBzK sample. Given the large number of objects in our sample, we were able to stack the radio continuum in bins of different galaxy properties, such as magnitude, color, and mass. Measured radio fluxes were converted to star formation rates using the median redshift of each stacked sample (1.7 for the whole population), a synchrotron emission spectral index of  $-0.8$ , and the conversion factor between radio luminosity and SFR from Yun et al. (2001), *i.e.*

$$\text{SFR} = 5.9 \pm 1.8 \times 10^{-22} L_{1.4\text{GHz}} (\text{M}_\odot/\text{yr}), \quad (1)$$

where  $L_{1.4\text{GHz}}$  is in  $\text{W Hz}^{-1}$ . Errors on SFRs are the squared sum of the uncertainties coming from the off-source rms in the stacked images, the fitting to recover total fluxes, and the uncertainty in equation (1).

In Figure 3 we show our results for the radio stacking of the AGN-cleaned sBzK sample as a function of: *i*) the observed B-band magnitude, which is related to the restframe dust uncorrected UV luminosity; *ii*) the  $(B-z)$  color, which for galaxies at  $z \sim 2$  is a proxy for the UV slope of the spectral energy distribution and hence it relates to dust extinction; and *iii*) the galaxy stellar mass. We conclude that: 1) overall, the emerging UV light is poorly correlated with the ongoing SFR, and –somewhat counter intuitively– the highest SFRs are found among the UV-faintest galaxies; 2) this happens because galaxies with higher SFRs are more extinguished in the UV; and 3) the SFR increases with stellar mass

almost linearly, as the slope of the  $\text{Log}(\text{SFR})$ - $\text{Log} M_*$  relation is  $0.95 \pm 0.07$ , in agreement (within the small errors) with the relation found by Daddi et al. (2007a).

#### 3.1. The specific star formation rate

In Figure 4 (left panel) we present radio derived specific star formation rates ( $\text{SSFR} = \text{SFR}/M_*$ ) for the reduced sBzK sample, divided in two redshift bins centered at  $z \approx 1.6$  (solid squares) and 2.1 (solid pentagons). From the observed B-band magnitudes we also derive  $\text{UV}_{1500}$  luminosities, uncorrected for dust attenuation, then estimating an uncorrected UV-derived SSFRs, which are also plotted in the same Figure with empty symbols. Some striking features are worth noting in the plot: *i*) the UV-derived SSFR drops dramatically with increasing mass whereas dust free SSFRs show no such effect, the SSFR being constant over almost one dex in mass (see also Dunne et al. (2009)); *ii*) correcting the UV light with a single value of extinction  $A_{1500}$  at all masses (an approximation often adopted in the literature, see e.g. Gabasch et al. 2004; Juneau et al. 2005; Bauer et al. 2005) would result in an artificial decreasing SSFR with increasing mass; and *iii*) the mean dust attenuation is a function of the galaxy stellar mass, with more massive galaxies being more dust-extinguished.

By taking advantage of the available photometric redshifts, we can split our sBzK sample in four redshift bins centered at  $z \approx [1.4, 1.6, 1.9, 2.3]$  and look for the redshift evolution of the SSFR, which is almost independent of stellar mass. On the right panel of Figure 4 we show how SSFRs are steadily increasing with redshift, by a factor  $\sim 4$  in the explored redshift range.

We also overplot three lower redshifts realizations (Brinchmann et al. 2004; Noeske et al. 2007; Elbaz et al. 2007) and the  $z \sim 2$  estimate by Daddi et al. (2007a), by computing the SSFR predicted from these studies for star forming galaxies with  $M_* \sim 3 \times 10^{10} \text{M}_\odot$ , and show how the SSFRs have decreased by a factor 40, for this mass galaxies, from  $z \approx 2.3$  all the way down to the local Universe.

#### 3.2. The dust attenuation at 1500 Å

By forcing the dust-corrected UV-SFRs to agree with the radio-SFRs, as both a function of galaxy stellar mass and  $(B-z)$  color, we obtain how the UV light attenuation  $A_{1500}$  at  $z \sim 2$  relates to these quantities. The result is shown in the inserts of Figure 5. Meurer et al. (1999) found a similar relation for a sample of local starburst galaxies. Our relation naturally extends their results to higher redshifts, and also nicely shows that the sBzK selection is much less biased against highly obscured objects than UV-selected samples. The latter ones are

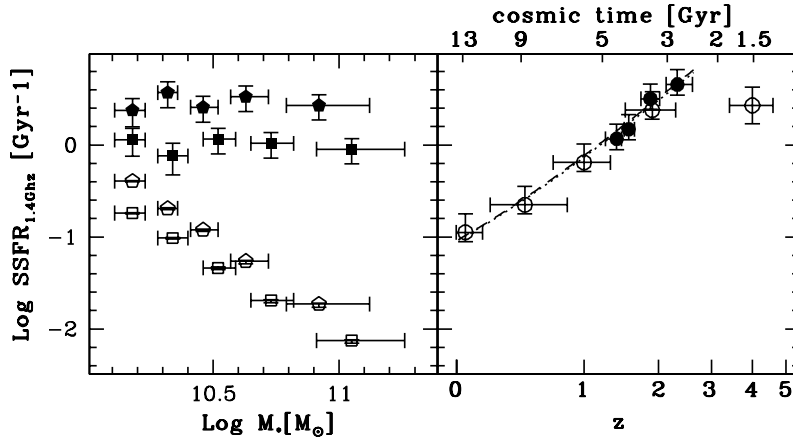


FIG. 4.— **Left:** Radio derived SSFR (solid symbols) at  $z \approx 1.6$  (squares) and  $\approx 2.1$  (pentagons) are compared to the uncorrected UV derived SSFR (empty symbols) as a function of  $\text{Log } M_*$ . **Right:** Radio derived SSFRs from this work (solid dots), for star forming galaxies with  $M_* \sim 3 \times 10^{10} M_\odot$ , as a function of redshift at  $z \approx 1.4, 1.6, 1.9, 2.3$ . Literature data are plotted as empty circles. The dotted curve shows the SSFR as a function of redshift described by equation (2).

indeed limited to moderate extinctions, such as  $A_{1500} < 3.6$  mag (Meurer et al. 1999).

In the explored redshift interval the dust attenuation, stellar mass and SFR are all tightly correlated with each other. The left panel of Figure 5 shows that the dust extinction  $A_{1500}$  tightly correlates with galaxy mass. Therefore, assuming a constant value for  $A_{1500}$  (independent of galaxy mass) introduces a systematic bias and the resulting  $\text{SSFR}(M_*)$  relation decreases with increasing stellar mass.

We emphasize the excellent agreement of the dust-attenuation correction here derived using the radio data with that derived from the UV continuum slope: the dotted line in the right panel of Figure 5 shows the relation between attenuation and  $(B-z)$  color predicted by the Calzetti et al. (1994) law, as calibrated in Daddi et al. (2004).

### 3.3. The Mass growth of galaxies

The present results confirm that, within the explored mass range, the SSFR of  $z \sim 2$  star-forming galaxies is almost independent of stellar mass (Daddi et al. 2007a; Dunne et al. 2009). A tight correlation between SFR and stellar mass was also found at  $z \sim 1$  (Elbaz et al. 2007),  $z = 0.2 - 0.7$  (Noeske et al. 2007) and  $z \sim 0$  (Brinchmann et al. (2004)). Other studies extensively discussed by Dunne et al. (2009) find instead a SSFR that declines appreciably with increasing stellar mass (see also Cowie & Barger 2008). In this respect, we concur with the arguments put forward by Dunne et al., that appear to be strengthened by our findings.

The SSFR secular decline and the mentioned results can be represented roughly by the relation:

$$\overline{\text{SFR}} \simeq 270 (M_*/10^{11} M_\odot) (t/3.4 \times 10^9 \text{yr})^{-2.5} (M_\odot/\text{yr}), \quad (2)$$

where  $t$  is the cosmic time.

We stress here that the exponent of  $M_*$  in equation (2) may not be strictly 1, and may depend on redshift (cf. Dunne et al. 2009), hence this relation is best valid for  $M_* \sim 3 \times 10^{10} M_\odot$  and  $z < 2.4$  ( $T > 2.7$  Gyr) for which it was derived. Still it represents a fair approximation for the star forming galaxy population. In Figure 4 we show that such a relation does not hold for the  $z \sim 4$  galaxies belonging to the Daddi et al. (2009) sample, this suggests that it has an important flattening above a certain redshift, qualitatively resembling in its behaviour the redshift evolution of the cosmic star formation history.

Integrating equation (2) from  $z=2$  to  $z=0$ , *i.e.* assuming that individual galaxies continued making stars and growing in mass all the way to low redshift, they would increase in mass by a factor  $\sim 250$ , a clear overgrowth even neglecting the contribution of merging events.

On the other hand, star-forming galaxies *do* form stars at these high rates, so either equation (2) is grossly erroneous, or at some point it ceases to apply to individual galaxies. Indeed, between  $z \sim 2.4$  and  $z \sim 0$  a major transformation takes place in the population of galaxies. While at  $z \sim 2.4$  only a small fraction of the stellar mass is in passively evolving galaxies (elliptical and bulges), this fraction grows up to  $\sim 60\%$  by  $z = 0$  (Baldry et al. 2004). Therefore, we argue that equation (2) does indeed apply to star-forming galaxies all the way to  $z = 0$ , but star formation turns off in a growing fraction of galaxies, which progressively turn into passive ellipticals and bulges. Mapping quantitatively this transformation goes beyond the scope of the present Letter.

## 4. CONCLUSIONS

We have presented first results of a study aimed to investigate the dust-unbiased star formation properties of high redshift galaxies, by focusing on their stacked radio properties. We use a sample of sBzK galaxies, drawn from the COSMOS survey, with a median redshift of 1.7, rejecting known AGN identified in both deep X-ray Chandra data and the 1.4 GHz radio imaging.

We demonstrate that a universal dust-attenuation correction cannot be applied to our sample. For instance, the generic factor of 5 often used to correct the UV light of Lyman-break galaxies (LBG) is applicable in our sample only for objects with  $M_* \sim 3 \times 10^{10} M_\odot$  –which incidentally is very close to the median stellar mass of LBG galaxies (Shapley et al. 2001)– but would grossly underestimate the correction for more massive galaxies.

We extend the results of Daddi et al. (2007a) that UV light, appropriately corrected, is a reliably tracer of SFR at  $z \sim 2$ .

We find that the SFR of star-forming galaxies increases almost linearly with stellar mass at all explored redshifts.

It appears that we are witnessing an evolution era when almost all star forming galaxies had the same evolutionary timescales and a nearly exponential growth, independent of

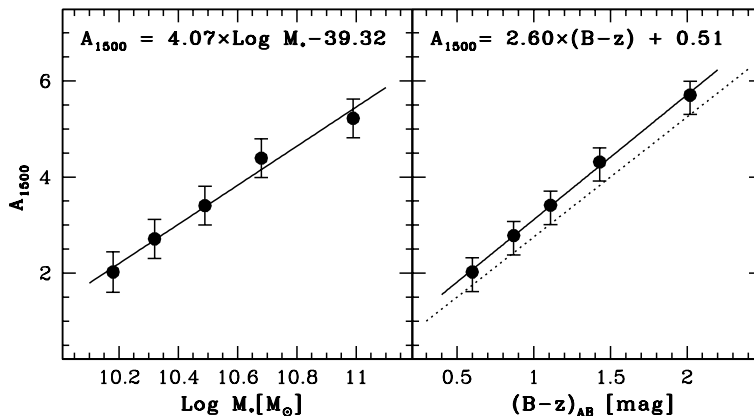


FIG. 5.— **Left:** UV light attenuation ( $A_{1500} = 2.5 \times \text{Log}(\text{SFR}_{1.4\text{GHz}}/\text{SFR}_{1500})$ ) as a function of galaxy stellar mass. **Right:** UV light attenuation as a function of B-z color (UV slope). The dotted line shows the attenuation law derived in Daddi et al. (2004) as described in the text.

mass. This is consistent with Dunne et al. (2009) results. They argue that the discrepancy found with literature studies might be due to selection biases present in UV and optically selected studies. While we agree with their statement, we point out that an underestimate of the dust attenuation correction could also explain such discrepancy.

We also find that the mass-independent SSFRs decrease by a factor 4 in the redshift range from  $z = 2.3$  to 1.4, a trend that continues all the way to the local Universe. Individual galaxies would enormously overgrow in mass if these empirical SFRs were maintained down to low redshifts. We suggest that this does not happen because many galaxies turn passive, and do so in a *downsized* fashion, because massive galaxies are first to reach unsustainable SFR levels. Thus, in massive starforming galaxies at  $z \sim 2$  downsizing has not started yet, but it will soon: we are just at the *dawn of downsizing*.

Constraining the nature of the physical processes by which SSFR are kept approximately constant in star forming galaxies of wildly different mass, and the mechanisms that contribute to discontinuing the star formation activity in massive

high redshift galaxies, are both substantial challenges for theoretical models to reproduce and for observers to investigate in full detail. New ideas on gas accretion modes (Dekel et al. 2009) and recent observations of widespread large molecular gas reservoirs (Daddi et al. 2008; Tacconi et al. 2008) in distant massive galaxies will likely provide crucial paths to understand these issues.

We thank the anonymous referee for constructive comments which improved the presentation of our results. MP, VS and CLC acknowledge partial support from the Max-Planck Forschungspreis 2005. ED and HJMcC acknowledge support from the French grants ANR-07-BLAN-0228-03 and ANR-08-JCJC-0008. AR acknowledges support from the ASI grant COFIS. This work is based in part on data products produced at TERAPIX. The HST COSMOS Treasury program was supported through NASA grant HST-GO-09822. We gratefully acknowledge the contributions of the entire COSMOS collaboration.

#### REFERENCES

- Baldry, I. K., Glazebrook, K., Brinkmann, J., et al. 2004, *ApJ*, 600, 681  
 Bauer, A. E., Drory, N., Hill, G. J., & Feulner, G. 2005, *ApJ*, 621, L89  
 Brinchmann, J., Charlot, S., White, S. D. M., et al. 2004, *MNRAS*, 351, 1151  
 Bundy, K., Ellis, R. S., & Conselice, C. J. 2005, *ApJ*, 625, 621  
 Capak, P., Aussel, H., Ajiki, M., et al. 2007, *ApJS*, 172, 99  
 Carilli, C. L., Murayama, T., Wang, R., et al. 2007, *ApJS*, 172, 518  
 Carilli, C. L., Lee, N., Capak, P., et al. 2008, *ApJ*, 689, 883  
 Condon, J. J. 1992, *ARA&A*, 30, 575  
 Condon, J. J., Cotton, W. D., & Broderick, J. J. 2002, *AJ*, 124, 675  
 Cowie, L. L. & Barger, A. J. 2008, *ApJ*, 686, 72  
 Cowie, L. L., Songaila, A., Hu, E. M., & Cohen, J. G. 1996, *AJ*, 112, 839  
 Daddi, E., Cimatti, A., Renzini, A., et al. 2004, *ApJ*, 617, 746  
 Daddi, E., Dickinson, M., Morrison, G., et al. 2007a, *ApJ*, 670, 156  
 Daddi, E., Alexander, D. M., Dickinson, M., et al. 2007b, *ApJ*, 670, 173  
 Daddi, E., Dannerbauer, H., Elbaz, D., et al. 2008, *ApJ*, 673, L21  
 Daddi, E., Dannerbauer, H., Stern, D., et al. 2009, *ApJ*, 694, 1517  
 Damen, M., Labbé, I., Franx, M., et al. 2009, *ApJ*, 690, 937  
 Davies, G. T., Gilbank, D. G., Glazebrook, K., et al. 2009, *MNRAS*, 395, L76  
 Dekel, A., Birnboim, Y., Engel, G., et al. 2009, *Nature*, 457, 451  
 Dickinson, M., Papovich, C., Ferguson, H. C., & Budavári, T. 2003, *ApJ*, 587, 25  
 Drory, N., Bender, R., Feulner, G., et al. 2004, *ApJ*, 608, 742  
 Dunne, L., Ivison, R. J., Maddox, S., et al. 2009, *MNRAS*, 394, 3  
 Elbaz, D., Daddi, E., Le Borgne, D., et al. 2007, *A&A*, 468, 33  
 Elvis, M., Civano, F., Vignali, C., et al. 2009, e-prints ArXiv:0903.2062  
 Erb, D. K., Steidel, C. C., Shapley, A. E., et al. 2006, *ApJ*, 647, 128  
 Feulner, G., Gabasch, A., Salvato, M., et al. 2005, *ApJ*, 633, L9  
 Fontana, A., Salimbeni, S., Grazian, A., et al. 2006, *A&A*, 459, 745  
 Gabasch, A., Salvato, M., Saglia, R. P., et al. 2004, *ApJ*, 616, L83  
 Garn, T. & Alexander, P. 2009, *MNRAS*, 394, 105  
 Ilbert, O., Capak, P., Salvato, M., et al. 2009, *ApJ*, 690, 1236  
 Juneau, S., Glazebrook, K., Crampton, D., et al. 2005, *ApJ*, 619, L135  
 Kennicutt, Jr., R. C. 1998, *ARA&A*, 36, 189  
 Marchesini, D., van Dokkum, P. G., Forster Schreiber, N. M., et al. 2008, e-prints ArXiv:0811.1773  
 Meurer, G. R., Heckman, T. M., & Calzetti, D. 1999, *ApJ*, 521, 64  
 Noeske, K. G., Weiner, B. J., Faber, S. M., et al. 2007, *ApJ*, 660, L43  
 Pannella, M., Hopp, U., Saglia, R. P., et al. 2006, *ApJ*, 639, L1  
 Peng, C. Y., Ho, L. C., Impey, C. D., & Rix, H.-W. 2002, *AJ*, 124, 266  
 Sadler, E. M., Jackson, C. A., Cannon, R. D., et al. 2002, *MNRAS*, 329, 227  
 Salpeter, E. E. 1955, *ApJ*, 121, 161  
 Schinnerer, E., Smolčić, V., Carilli, C. L., et al. 2007, *ApJS*, 172, 46  
 Scoville, N., Aussel, H., Brusa, M., et al. 2007, *ApJS*, 172, 1  
 Shapley, A. E., Steidel, C. C., Adelberger, K. L., et al. 2001, *ApJ*, 562, 95  
 Smolčić, V., Schinnerer, E., Scoddeggio, M., et al. 2008, *ApJS*, 177, 14  
 Smolčić, V., Schinnerer, E., Zamorani, G., et al. 2009a, *ApJ*, 690, 610  
 Smolčić, V., Zamorani, G., Schinnerer, E., et al. 2009b, e-prints ArXiv:0901.3372  
 Tacconi, L. J., Genzel, R., Smail, I., et al. 2008, *ApJ*, 680, 246  
 Thompson, A. R. 1999, in *Astronomical Society of the Pacific Conference Series*, Vol. 180, *Synthesis Imaging in Radio Astronomy II*, ed. G. B. Taylor, C. L. Carilli, & R. A. Perley  
 White, R. L., Helfand, D. J., Becker, R. H., Glikman, E., & de Vries, W. 2007, *ApJ*, 654, 99  
 Yun, M. S., Reddy, N. A., & Condon, J. J. 2001, *ApJ*, 554, 803  
 Zheng, X. Z., Bell, E. F., Papovich, C., et al. 2007, *ApJ*, 661, L41